Macromolecular Rapid Communications
www.mrc-journal.de

A Hyperbranched Phosphorus/Nitrogen/Silicon-Containing Polymer as a Multifunctional Additive for Epoxy Resins

Qian Zhong, Siqi Huo, Cheng Wang, Guofeng Ye, Qi Zhang, Hao Wang, and Zhitian Liu**

High-performance, versatile epoxy resins (EPs) are used in a variety of fields, but the manufacture of transparent, fireproof, and strong EPs remains a major challenge. The hyperbranched, multifunctional flame retardant (DSi) is prepared by using diethanolamine, polyformaldehyde, diphenylphosphine oxide, and phenyltrimethoxysilane as raw materials in this work. When the additional amount of DSi is only 2 wt.%, the EP-DSi$_2$ sample reaches a vertical burning (UL-94) V-0, and its limiting oxygen index (LOI) is 32.8%. When the content of DSi is 3 wt.%, the peak heat release rate (PHRR) and total smoke production (TSP) of EP-DSi samples are 43.8% and 21.4% lower than those of EP. The good compatibility of DSi and EP endows EP-DSi with high transparency, and the hyperbranched structure of DSi makes EP-DSi have obviously enhanced mechanical strength and toughness. The enhanced fire safety of EP-DSi is mainly due to the promoting carbonization and radical quenching effects of DSi. This paper offers a comprehensive design concept aimed at creating high-performance epoxy resins with good optical, mechanical, and flame-retardant properties, which have broad application prospects.

1. Introduction

EP has been extensively utilized across diverse industries due to its superior chemical resistance, electrical insulation, mechanical strength, and thermal stability. However, because it EP a flammable polymer, it is easy to ignition and will produce toxic fumes when burned, which limits its application.[1–5] The fire safety of polymers can be improved by adding flame retardants.[6,7] The halogenated flame retardants have been proven to be effective in enhancing the flame-retardant properties of polymers, but they will produce a lot of toxic smoke during combustion.[8–11] Currently, phosphorus (P)-based flame retardants serve as alternatives to halogen-containing ones due to their high flame retardant effects.[12–14]

Different flame-retardant elements have been utilized as the synergists for phosphorus, e.g., nitrogen (N) and silicon (Si).[15–17] For instance, Li et al.,[18] prepared a P/Si-containing flame retardant (DPSi-ED) and introduced it into the EP system to enhance flame retardancy. It was found that the resultant EP showed an LOI of 35.3% and a UL-94 V-0 classification. Chai et al.,[19] prepared a P/Si/N-containing hyperbranched polymer (Si-DP). When the P content of EP/Si-DP was 1.1 wt.%, it reached a UL-94 V-0 rating and its LOI was 33.9%. Meanwhile, EP/Si-DP retained high transparency and showed an increased glass transition temperature (T_g). Clearly, the synergistic flame-retardant action of phosphorus, nitrogen, and silicon in the condensed phase effectively suppressed the heat release and smoke production, thereby enhancing fire safety.[18,20–22] Hu et al.,[23] synthesized a phosphorous/nitrogen-containing flame retardant (HPNFR) by using dimethyl methylphosphonate and tri (2-hydroxyl ethyl) isocyanurate as raw materials. The cone calorimetry test results indicated that the EP/HPNFR sample showed lower heat and smoke release than EP.

However, EP is a highly cross-linked thermoset, so it suffers from poor toughness, but fortunately, hyperbranched polymers can solve this problem, because of its unique intramolecular cavity and branched structure.[5,16,24] For instance, Tang et al.,[25] synthesized a novel P/N-based hyperbranched epoxy resin, which can effectively enhance the impact strength, tensile strength, and bending strength of EP by 53.9%, 29.2%, and 58%, respectively, relative to pure EP. These results proved that hyperbranched polymers can effectively enhance the toughness of EP.

Q. Zhong, C. Wang, G. Ye, Q. Zhang, Z. Liu
Hubei Engineering Technology Research Center of Optoelectronic and New Energy Materials
School of Materials Science & Engineering
Wuhan Institute of Technology
Wuhan 430205, China
E-mail: able.ztliu@wit.edu.cn

S. Huo, H. Wang
Centre for Future Materials
School of Engineering
University of Southern Queensland
Springfield 4300, Australia
E-mail: Siqi.Huo@unisq.edu.au

The ORCID identification number(s) for the author(s) of this article can be found under https://doi.org/10.1002/marc.202400801

[The copyright line for this article was changed on 24 February 2025 after original online publication.]

DOI: 10.1002/marc.202400801

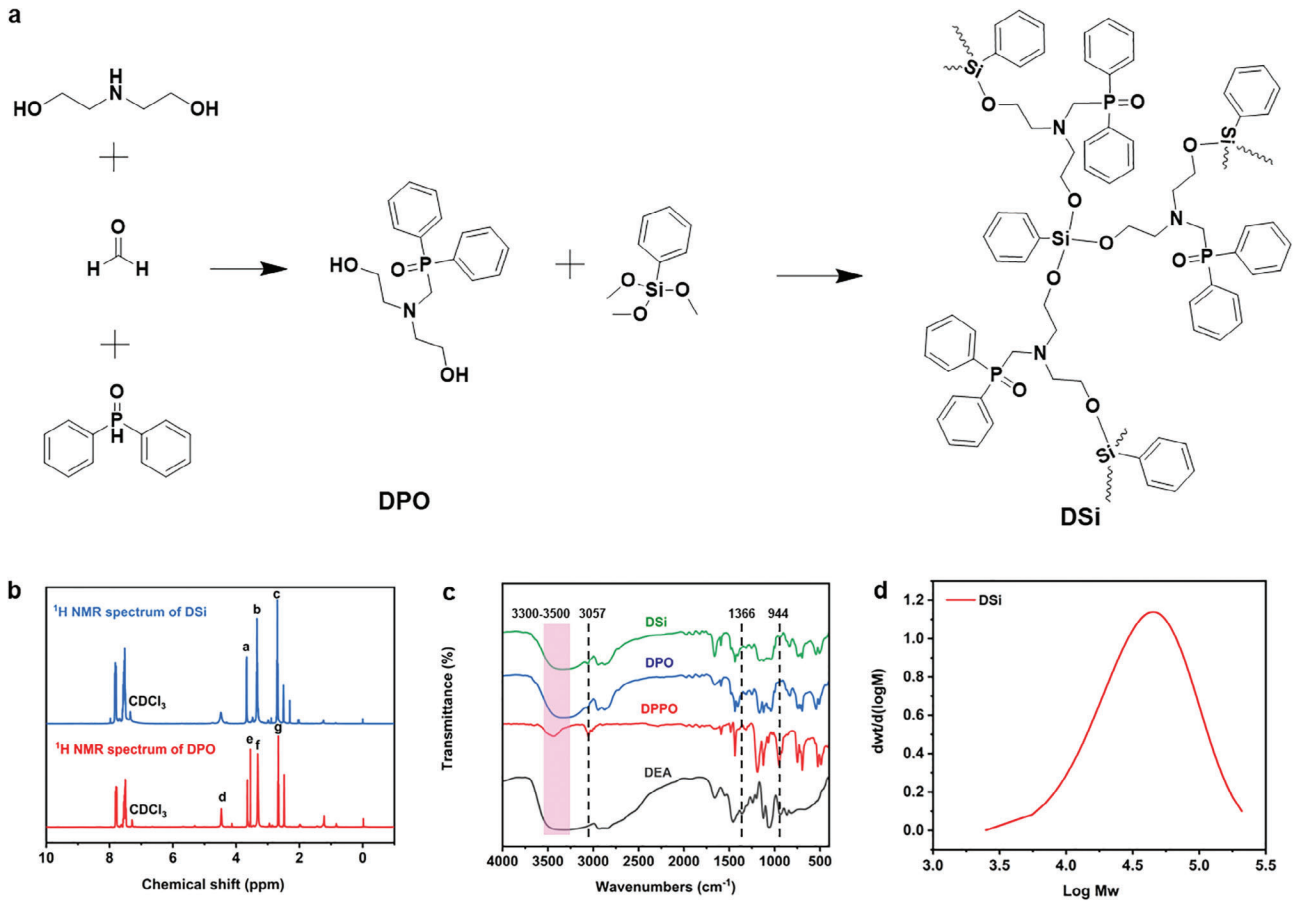

Figure 1. a) Schematic of the synthesis procedure for DSi; b) ^{1}H NMR spectra of DPO and DSi; c) FTIR spectra of DEA, DPPO, DPO, and DSi; and d) GPC curve of DSi.

However, these P-containing flame retardants and hyperbranched polymers usually needed high loading levels to enhance flame retardancy and toughness of EP. Introducing a large number of additives will significantly reduce the optical properties and thermal stability of EP.[26] Thus, the fabrication of transparent, high-performance EPs combining great thermal stability, fire safety, and mechanical properties using a handful of additives is still an enormous challenge.

In this work, a hyperbranched P/Si/N-containing flame retardant (DSi) was synthesized by using diethanolamine, polyformaldehyde, diphenylphosphine oxide, and phenyltrimethoxysilane as raw materials, and its chemical structure was characterized in detail. Subsequently, the impacts of DSi on the optical properties, mechanical properties, thermal stability, and fire safety of EP were evaluated, followed by in-depth toughening and flame-retardant mechanism analyses.

2. Results and Discussion

2.1. Characterization of DSi

DPO was synthesized by the reaction of DEA, polyformaldehyde, and DPPO, and then DPO and PTMS were used as raw materials to synthesize DSi (**Figure 1a**). The chemical structure of DSi was analyzed by nuclear magnetic resonance (NMR), Fourier infrared spectroscopy (FTIR), and gel permeation chromatography (GPC) techniques, with the results illustrated in Figure 1b–d and Figure S1 (Supporting Information). In the ^{1}H NMR of DPO (Figure 1b), the signal of P-H disappeared at 8.85 ppm, and that of aldehyde disappeared at 11.53 ppm.[16,27] After the reaction between DPO and PTMS, the signal of —OH at 4.46 ppm in ^{1}H NMR of DSi weakened, and only one peak can be observed at 26.9 ppm in the ^{31}P NMR of DSi (Figure S1, Supporting Information), indicating the successful synthesis of DSi. In the FTIR spectra of DSi, DPO, and DEA (Figure 1c), the absorption bands of —OH appeared at 3300–3500 cm^{-1}.[9,28] The absorption peak of Ph-H can be detected at 3057 cm^{-1} in the FTIR spectra of DSi, DPO, and DPPO.[16] For DSi, the characteristic peak of Si—Ph appeared at 1366 cm^{-1},[29] and that of Si—O—C was located at 944 cm^{-1}.[30] The GPC trace of DSi is presented in Figure 1d. The numerical average molecular weight (M_n) of DSi was 27 811 g mol^{-1}, and the polydispersity index was 1.88. All these results confirm that the phosphorus/silicon-containing hyperbranched DSi has been successfully synthesized.

2.2. Enhanced Char-Forming Ability

Thermogravimetric analysis (TGA) was performed in nitrogen and air conditions, respectively, to investigate the thermal stabil-

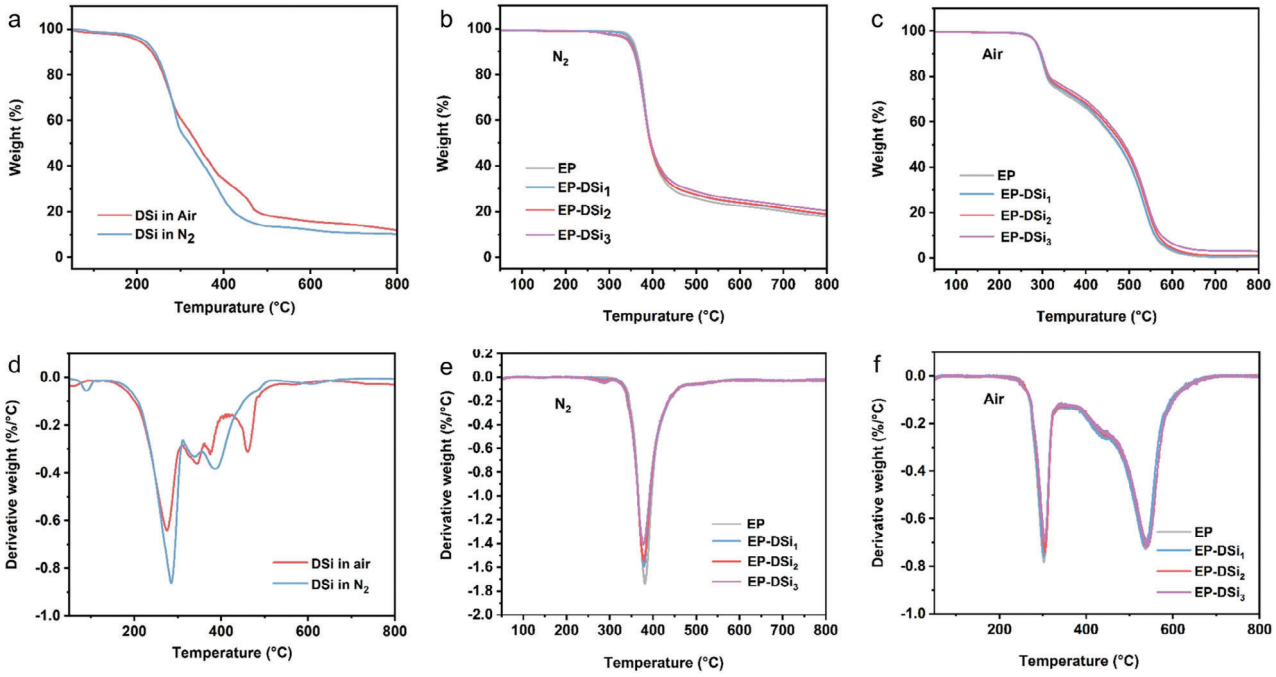

Figure 2. a) TG curves of DSi; TG curves of EP samples under b) N_2 and c) air atmosphere; d) DTG curves of DSi; and DTG curves of EP samples under (b) N_2 and (c) air atmosphere.

ity of DSi and EP-DSi, with the TG and derivative TG (DTG) plots presented in **Figure 2**. The thermal stability parameters, including initial decomposition temperature ($T_{5\%}$), the temperature at maximum weight loss rate (T_{max}), and char yield at 800 °C (CY) are listed in Table S2 (Supporting Information). The $T_{5\%}$ values of DSi under air and nitrogen atmosphere were 203 and 216 °C, (Figure 2a,c; Table S2, Supporting Information) and they were higher than the curing temperature of EP-DSi, indicating that DSi did not degrade during curing. In nitrogen condition, the main thermal decomposition of both EP and EP-DSi occurred from 300 to 500 °C (Figure 2b,e).[31] Under air atmosphere, both EP and EP-DSi showed a two-step thermal degradation, including the breakdown of the cross-linked network and oxidative decomposition of char residue occurred from 300 to 500 °C (Figure 2c,f).[32,33] Obviously, introducing a small amount of DSi did not reduce the initial decomposition temperatures of EP-DSi samples and influence the decomposition behaviors of EP-DSi samples.[34] The CY values of DSi samples reached 10.3% and 11.9% under nitrogen and air atmosphere, and those of EP were gradually increased with increasing loading level of DSi. Under the N_2 atmosphere, the CY of EP-DSi_3 was raised from 10.9 wt.% of EP to 20.5 wt.%, with an 86.2% enhancement. In air condition, the CY of EP-DSi_3 (3.0 wt.%) was 6.5 times higher than that of EP (0.4 wt.%). These results prove that incorporating DSi does not reduce the thermal stability of EP-DSi samples, but improves the carbonization ability, which is beneficial to its flame retardancy.[30,35]

2.3. Well-Preserved Optical Properties

The excellent optical properties of EP materials allow them to find wide applications in the optical field. The optical properties of EP and EP-DSi samples were evaluated by digital camera and UV–vis spectrophotometry. The transmittance of EP, EP-DSi_1, EP-DSi_2, and EP-DSi_3 at the wavelength of 800 nm was 84.7%, 84.6%, 83.3%, and 83.3%, respectively (**Figure** 3a,b). Thus, adding a small amount of DSi has little impact on the transparency of EP. The high transparency of EP-DSi samples can also be confirmed by their digital images in Figure 3d, and their film colors were close to that of EP film. At a low addition amount, DSi can be evenly distributed in the EP matrix, thus its addition does not affect the optical properties of EP-DSi samples. The EP-DSi samples with well-preserved optical properties can be widely applied in the optical device.[36] The amorphous nature of epoxy resins is the main reason for their high transparency.[32,37] Hence, the impact of DSi on the non-crystalline characteristic of EP was investigated using X-ray diffraction (XRD). All samples only had a wide diffraction peak near $2\theta = 18°$ (Figure 3c). Adding DSi has no effect on the amorphous property of EP, and thus the EP-DSi sample can maintain high transparency.

2.4. Outstanding Mechanical Properties

Mechanical tests, both dynamic and static, were performed on EP and EP-DSi samples to investigate how DSi influences the mechanical characteristics of the EP matrix. The results of dynamic mechanical analysis (DMA), including storage modulus (E') and tan delta plots, for EP and EP-DSi samples are illustrated in **Figure** 4a,b, with the data detailed in Table S3 (Supporting Information). The crosslinking density (υ) of EP is calculated according to the following equation: $\upsilon = E/3RT$, where R represents the gas constant and E is the E' at the temperature (T) 30 °C higher than T_g.[38,39] As presented in Figure 4b and Table S3 (Supporting Information), the T_g of EP-DSi was close

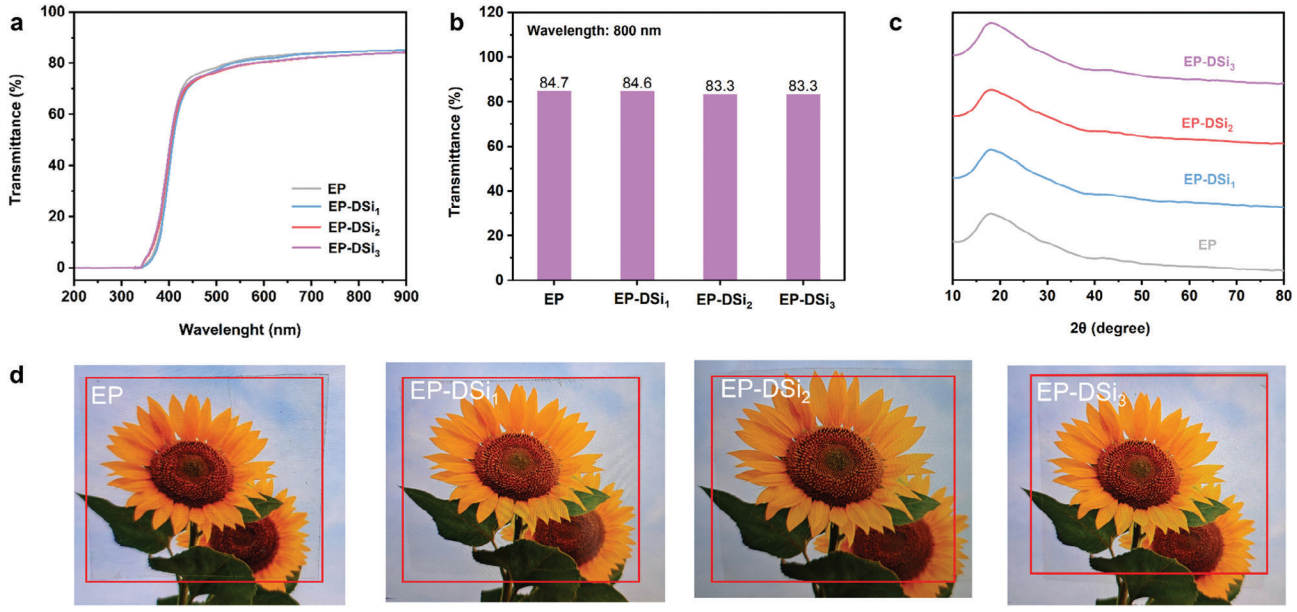

Figure 3. a) UV–vis absorption spectra of EP and EP-DSi samples; b) transmittance of EP and EP-DSi samples at the wavelength of 800 nm; c) X-ray diffraction patterns of EP and EP-DSi samples; and d) digital images of EP and EP-DSi samples.

to that of EP, but reduced gradually with the increase of DSi content. This can be attributed to the decreased crosslinking density and the presence of numerous voids in DSi, which facilitate the chain segment motion within the EP matrix.[39] The mechanical properties of EP and EP-DSi samples are displayed in Figure 4c–f and Table S4 (Supporting Information). The incorporation of DSi enhanced the mechanical performances of EP-DSi samples, and EP-DSi_2 containing 2 wt.% of DSi showed the best mechanical properties among all samples. As displayed in Figure 4c–e, the tensile strength, elongation at break, and tensile toughness of EP-DSi_2 reached 70.7 MPa, 6.0%, and 2.4 MJ m^{-3}, which were 14.4%, 71.4%, and 100% higher than those of EP (61.8 MPa, 3.5%, and 1.2 MJ m^{-3}). The mechanical properties of EP-DSi_3 were worse than those of EP-DSi_2, but better than those of EP. The impact strength of EP and EP-DSi is presented in Figure 4f. The impact strength was increased with increasing DSi addition. EP-DSi_3 exhibited an impact strength of 11.2 kJ m^{-2}, which was 220% higher than that of EP (3.5 kJ m^{-2}). These results confirm that DSi improves both the mechanical strength and toughness of EP.

The fracture surface of the sample after the impact test was tested by scanning electron microscopy (SEM). The EP surface was smooth and showed a regular crack (Figure 4g), indicative of a brittle fracture. However, the EP-DSi surface was very rough, with many folds and shear bands (Figure 4h,i), demonstrating the improved toughness. DSi is a hyperbranched flame retardant, and there are many cavities within its chemical structure. These cavities can absorb a large amount of fracture energy, resulting in energy dissipation and improved toughness.[38]

2.5. Superior Fire Safety

To investigate the fire safety of EP samples, the LOI, UL-94, and cone calorimetric tests were carried out, with the results shown in **Figure 5** and Tables S5 and S6 (Supporting Information). EP exhibited a low LOI value of 26.7% and failed the UL-94 test (Table S5, Supporting Information). The LOI value and UL-94 rating of EP-DSi demonstrated notable enhancements because of adding DSi. When DSi content reached 2 wt.%, EP-DSi_2 successfully achieved a UL-94 V-0 rating and an LOI value of 32.8%. The results confirm that EP-DSi can achieve superior flame retardancy when a small amount of DSi is added. The addition of DSi increased the time to ignition (TTI) of EP-DSi during cone calorimetry testing. Specifically, the TTI increased from 70 s for pure EP to 78 s for EP-DSi_3 (Table S6, Supporting Information). This indicates that the decomposition products of DSi have an inhibitory effect on the ignition of EP. Furthermore, Figure 5a,b clearly demonstrate that incorporating DSi significantly reduces both the peak heat release rate (PHRR) and total heat release (THR) of EP-DSi. Compared to pure EP, the PHRR and THR values of EP-DSi_3 were reduced by 43.8% and 19.8%, respectively. This further confirms the effectiveness of DSi in enhancing the flame-retardant properties of EP.

The fire safety of materials can be assessed by using the fire growth rate (FIGRA) and fire performance index (FPI) (Figure 5c). The increase in FPI and the decrease in FIGRA demonstrate the improved fire safety.[32] The FPI and FIGRA of EP were 0.053 $m^2 s\ kW^{-1}$ and 8.74 kW $m^{-2}\ s^{-1}$, respectively, while those of EP-DSi_3 were 0.11 $m^2 s\ kW^{-1}$ and 4.91 kW $m^{-2}\ s^{-1}$, suggesting that DSi can effectively enhance the fire safety of EP at a low addition amount. Smoke generation poses a critical threat to life safety in a fire, and thus it is necessary to evaluate the smoke suppression of materials.[40,41] The smoke suppression performances of EP-DSi samples can be effectively enhanced by incorporating a small amount of DSi, as evidenced by their lower peak smoke production rate (PSPR) and total smoke production (TSP) values than those of EP (Figure 5d,e). The average effective heat of combustion (AEHC) can assess the combustion degree of volatile gases in the burning process. From Figure 5f, there was a decrease in the AEHC value as the DSi content increased, sug-

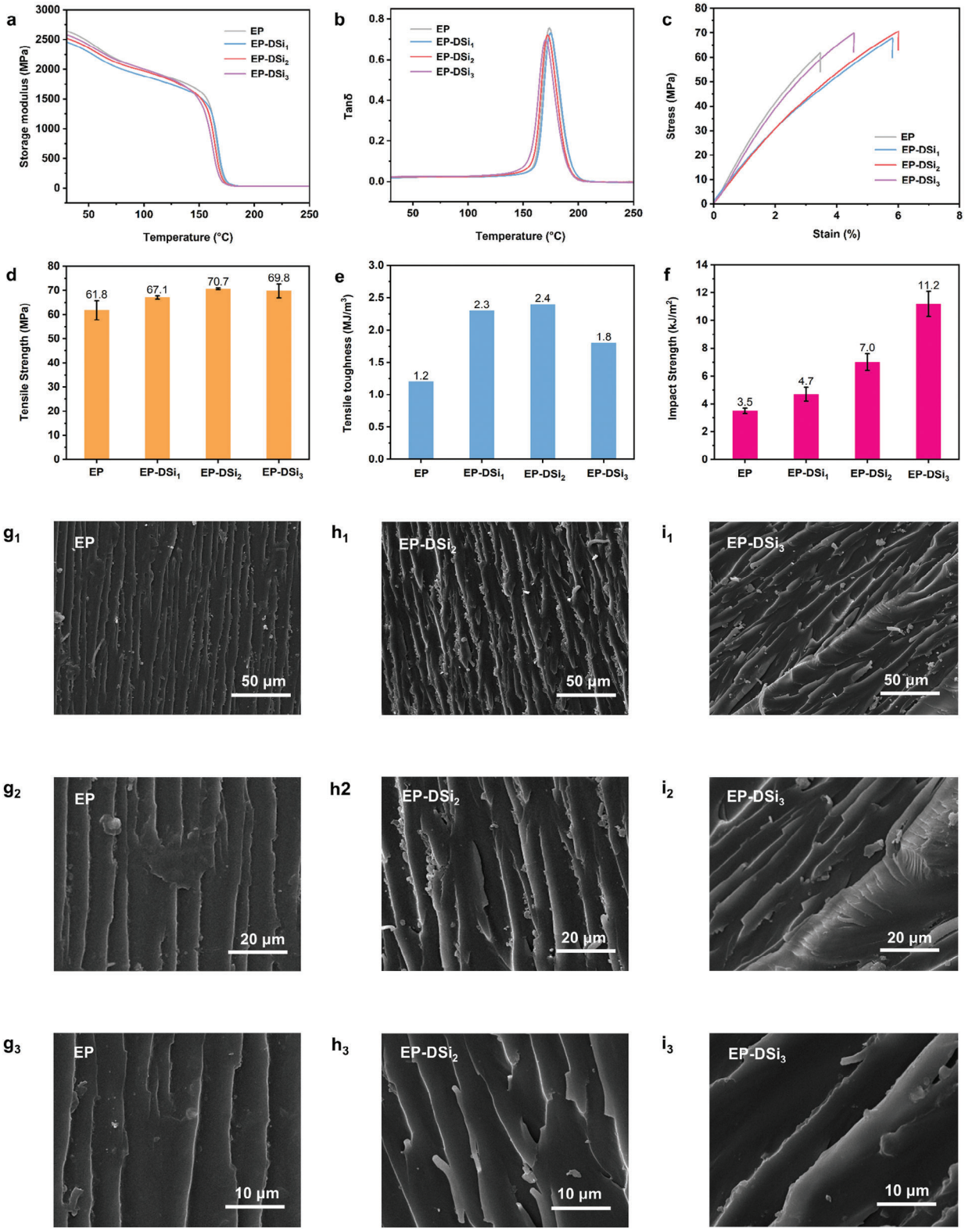

Figure 4. a) Storage modulus, b) tan delta, and c) tensile stress-strain plots of EP samples; d) tensile strength, e) tensile toughness, and f) impact strength of EP samples; and SEM cross-section images of (g_1-g_3) EP, (h_1-h_3) EP-DSi$_2$, and (i_1-i_3) EP-DSi$_3$ samples under different magnifications obtained from impact tests.

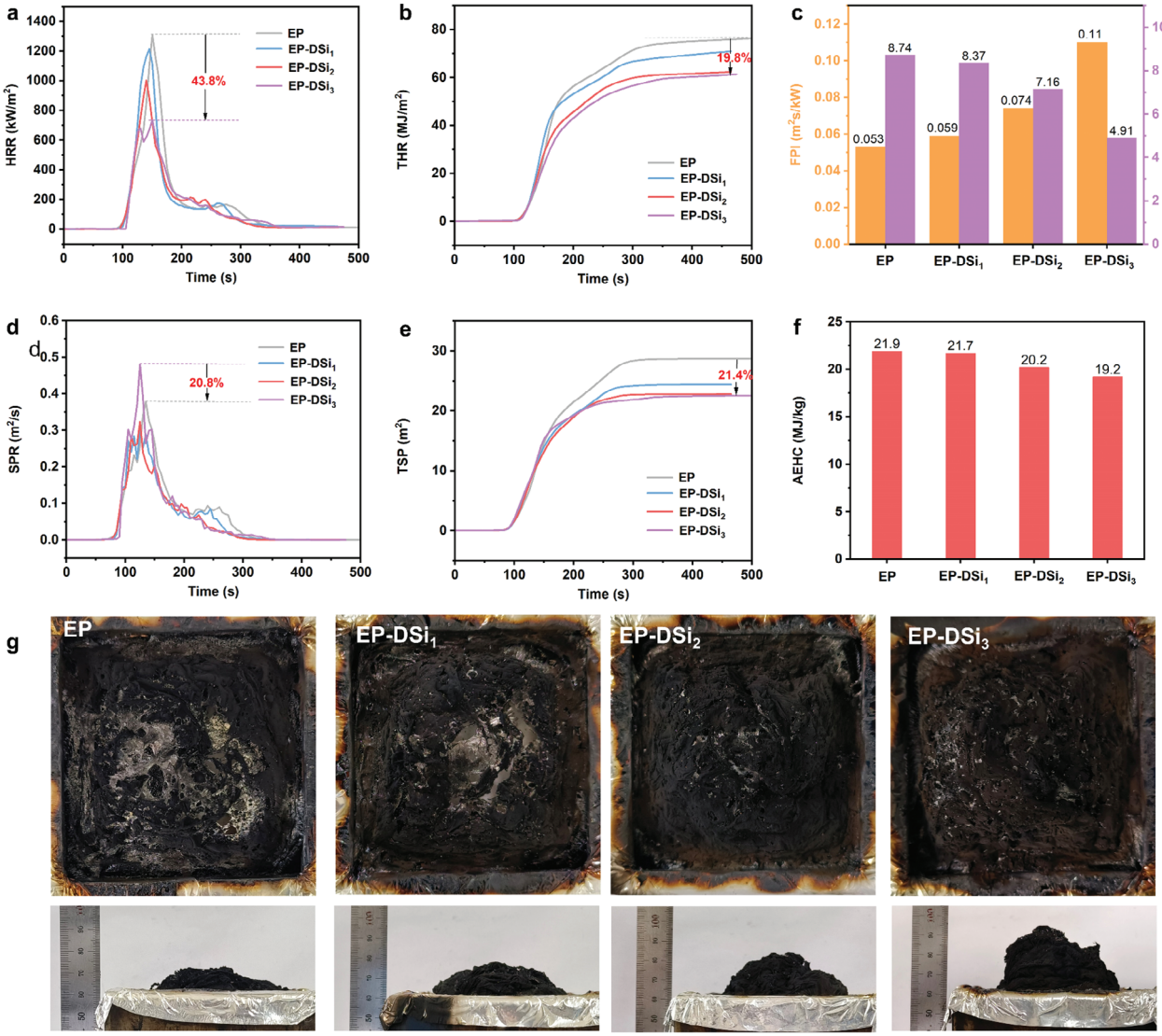

Figure 5. a) Heat release rate curves, b) total heat release plots, c) fire performance index and fire growth rate (FIGRA), d) smoke production rate plots, e) total smoke production curves, f) average effective heat of combustion of EP samples, and g) digital images of the chars after cone calorimetry.

gesting that the decomposition products of DSi can also exert the flame-retardant function in the gas phase.[37]

The digital photos of the residues obtained from cone calorimetric tests are shown in Figure 5g. The EP-DSi chars are much more than the EP char. The char expansion rate and surface continuity were increased as the DSi content increased. Obviously, the decomposition products of DSi promoted the carbonization of the EP matrix during combustion, which can retard heat release and smoke emission. Thus, the gas- and condensed-phase functions of DSi allowed EP to achieve superior fire safety.

2.6. Fire-Retardant Mode-of-Action Analysis

2.6.1. Condensed-Phase Analysis

SEM was used to study the micro-morphology of residual char obtained from the cone calorimetric test (see **Figure** 6a1–c1). Clearly, the EP residue exhibited a loose and powdery surface with many holes, which cannot suppress the heat and smoke release (Figure 6a1,a2). The surface consistency of EP-DSi residue was much higher than that of EP residue (Figure 6b1,b2,c1,c2), and the EP-DSi_3 char displayed a compact surface, which contributed to suppressing the combustion reaction.[42] The laser Raman spectrometer was utilized to investigate the flame-retardant mode-of-action of DSi in the condensed phase (Figure 6a3–c3). The D peak at 1364 cm^{-1} was attributed to the amorphous C atoms and the G peak at 1605 cm^{-1} was assigned to the graphitized C atoms. The area ratio between the D peak to the G peak (I_D/I_G) reflects the graphitization of the char layer, which is inversely proportional to the graphitization.[43,44] The I_D/I_G values of EP, EP-DSi_2, and EP-DSi_3 were 3.03, 2.81, and 2.75, respectively, demonstrating the positive effect of DSi on the carbonization of the EP matrix. Therefore, the degradation products of DSi in the condensed phase can improve the char-forming ability of EP, which was beneficial to retarding the burning reaction.[45]

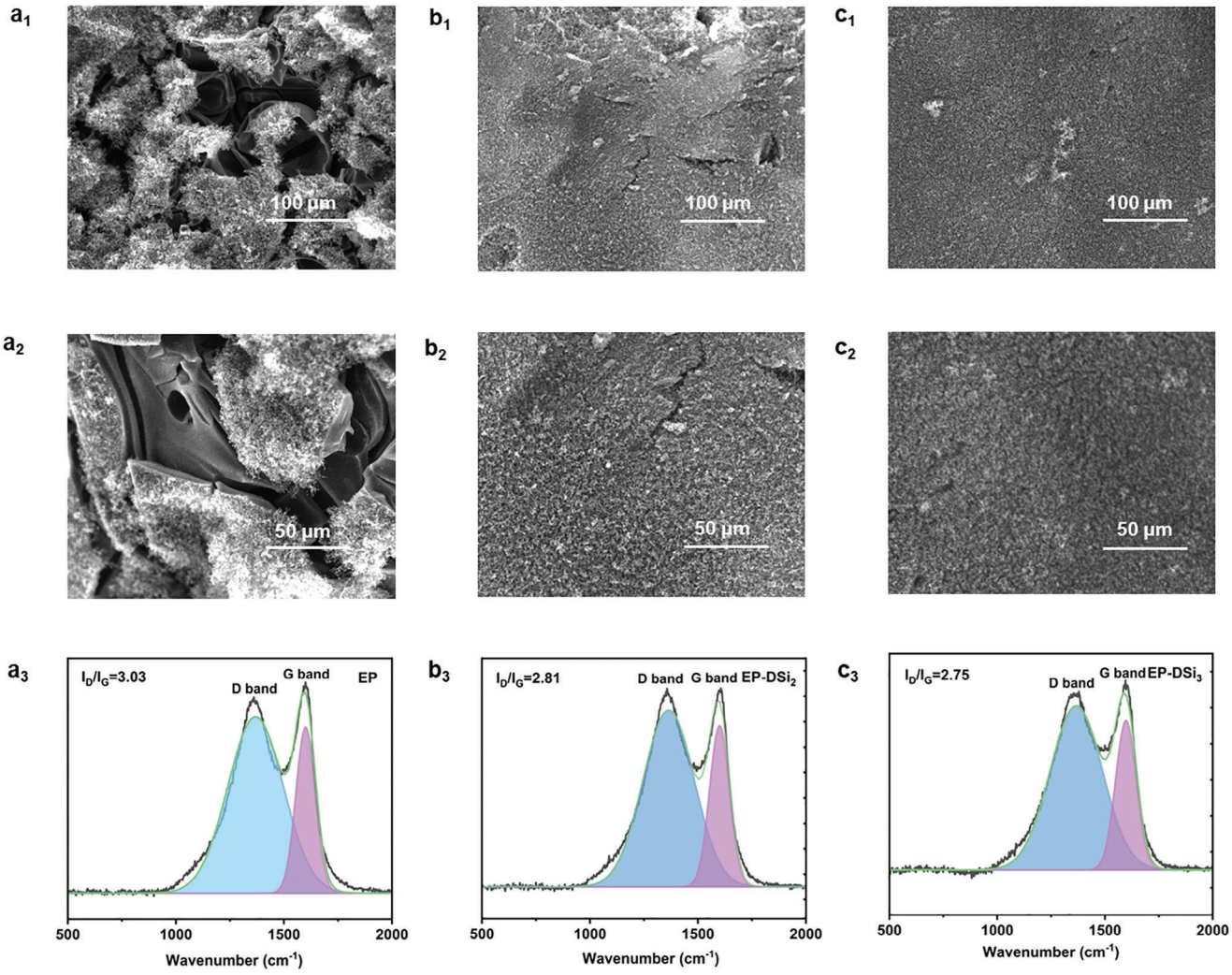

Figure 6. SEM images and Raman spectra char residues from cone calorimetry tests: a) EP, b) EP-DSi_2, and c) EP-DSi_3.

The residual char of EP-DSi_3 after the cone calorimetry test was tested by X-ray photoelectron spectroscopy (XPS) to study its chemical composition (**Figure 7**; Table S7, Supporting Information). EP-DSi_3 residue mainly contained C, N, O, P, and Si elements (Figure 7a). Based on the P and Si contents of EP-DSi_3 and its residue, it can be found that abundant P- and Si-containing decomposition products of DSi remained in the condensed phase (Table S7, Supporting Information). In the C1s spectrum, the deconvolution peaks associated with C—C, C—O, and C═O bonds can be observed at 284.7, 285.6, and 288.5 eV, respectively (Figure 7b).[46,47] The structures of C—N═C and pyridine-N- were responsible for the peaks at 398.4 and 400.0 eV in the N1s spectrum (Figure 7c).[37] Two deconvolution peaks at 531.7 and 533.6 eV can be detected in the O1s spectrum, corresponding to the O═C and O—C structures, respectively (Figure 7d). In addition, the peak at 133.7 eV in the P2p spectrum belonged to the P—O—C structure, and that at 102.9 and 101.5 eV in the Si2p spectrum belonged to the Si—O and Si—C structures (Figure 7e,f).[18,48] These results further indicate that the phosphate- and silicon-based fragments produced by DSi participate in the formation of a compact and intumescent char during combustion, thus inhibiting the heat and smoke release in the condensed phase.[22,49,50]

2.6.2. Gas-Phase Analysis

To investigate the gas-phase mode-of-action of DSi, the thermogravimetric analysis/infrared spectroscopy (TG-IR) was carried out on EP and EP-DSi_3 (**Figure 8**a–f). EP and EP-DSi_3 generated similar gaseous products under heating. These included water (3650 cm^{-1}), hydrocarbons (2972 cm^{-1}), CO_2 (2329 cm^{-1}), compounds with carbonyl groups (1750 cm^{-1}), aromatic compounds (1603 and 1511 cm^{-1}), compounds containing C—N bonds (1250 cm^{-1}), and ethers (1172 cm^{-1}).[16,51] EP-DSi_3 exhibited a slight increase in the peak intensity at 745 cm^{-1} compared to EP (Figure 8d), which can be attributed to the release of NH_3 gas during the thermal degradation of DSi. The promoting carbonization

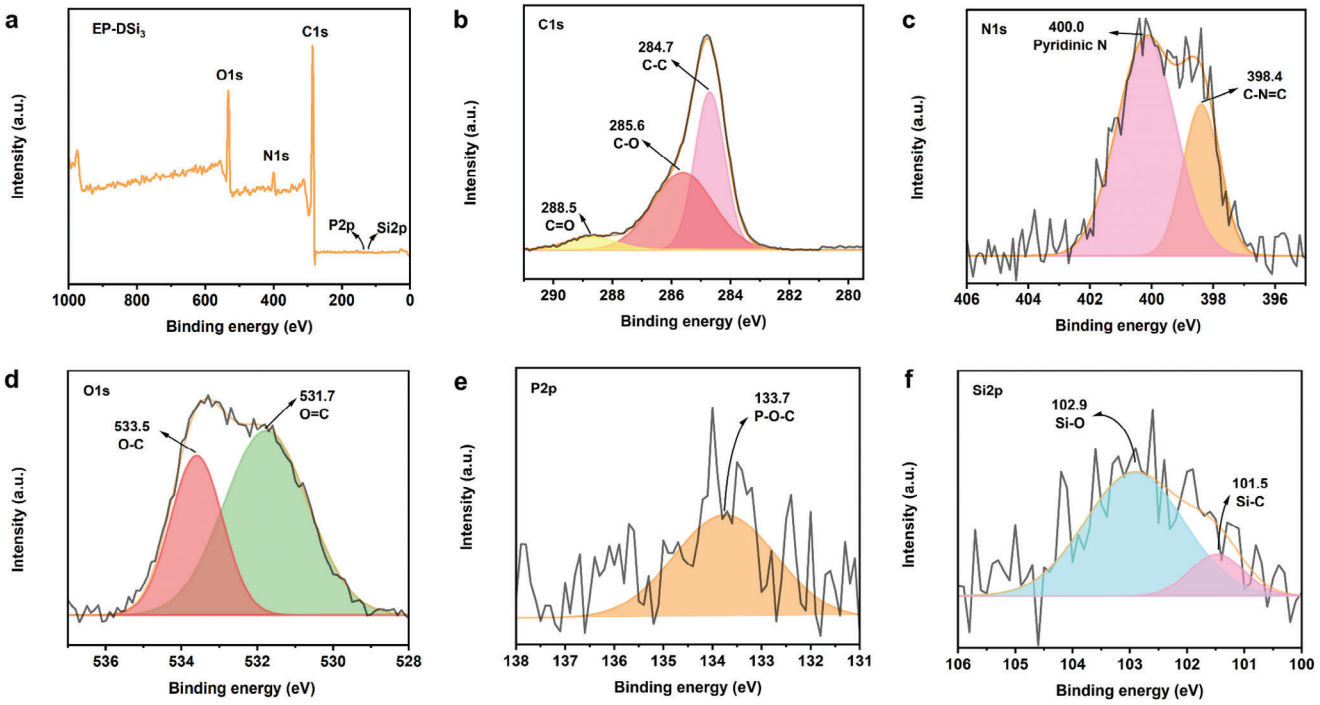

Figure 7. XPS a) full-scan and high-resolution b) C1s, c) N1s, d) O1s, e) P2p, and f) Si2p spectra of EP-DSi_3 residue.

effect of DSi led to the reduced intensity of aromatic compounds peak (Figure 8e). Moreover, EP-DSi_3 displayed decreased CO_2 generation relative to EP, which might be also attributed to the promoting carbonization effect of DSi. The pyrolysis behavior of DSi was studied using pyrolysis-gas chromatography/mass spectrometry (Figure 8g,h). The main pyrolysis products of DSi included aromatic fragments, DEA derivatives, and DPPO derivatives. The formation of these pyrolysis fragments was accompanied by the production of phosphorus-containing radicals. The phosphorus-based radicals can effectively capture the high-energy radicals during combustion, thus suppressing the burning reaction in the gaseous phase.[52–55] Hence, DSi functioned in both condensed and gaseous phases to suppress heat transfer and smoke generation during combustion.

3. Conclusion

A hyperbranched flame retardant (DSi) was produced by using diethanolamine, polyformaldehyde, diphenylphosphine oxide, and phenyltrimethoxysilane in this work. With a low addition amount (≤3 wt.%), DSi can significantly enhance the flame retardancy, smoke suppression, and mechanical properties of EP, and effectively maintain the optical performances. 2 wt.% of DSi can allow EP-DSi_2 to achieve a UL-94 V-0 rating and an LOI of 32.8%. Meanwhile, the introduction of DSi effectively reduced the PHRR and PSPR of the EP-DSi sample. Thus, DSi can simultaneously enhance flame retardancy and smoke suppression of EP by its gas- and condensed-phase flame-retardant effects. The tensile strength, elongation at break, and tensile toughness of EP-DSi_2 reached 70.7 MPa, 6.0%, and 2.4 MJ m^{-3}, which were 14.4%, 71.4%, and 100% higher than those of EP, confirming the reinforcing and toughening functions of DSi. Moreover, the visible light transmittance of EP-DSi was comparable to that of EP. Hence, the well-designed DSi can serve as a multifunctional additive to enhance the overall property of epoxy resin.

4. Experimental Section

Materials: Diglycidyl ether of bisphenol-A (DGEBA, CYD-127, epoxide equivalent weight: ≈185 g/equiv) was provided by Yueyang Baling Petrochemical Co., Ltd (Hunan, China). Diethanolamine (DEA), polyformaldehyde, diphenylphosphine oxide (DPPO), *N*,*N*-dimethylformamide (DMF), phenyltrimethoxysilane (PTMS), and diaminodiphenylmethane (DDM) were purchased from Energy Chemical Co., Ltd. (Shanghai, China).

Synthesis of DSi: The synthesis route of DSi is shown in Figure 1a. The intermediate (DPO) was synthesized in accordance with a previous work.[27] DPO was first vacuum-dried at 80 °C for 2 h, and then it was mixed with PTMS at a molar ratio of 3:1 in DMF. The mixture was continuously stirred for 6 h at 120 °C under a nitrogen atmosphere. After that, the mixture was distilled under vacuum at 140 °C for 2 h to remove DMF, and it was further dried at 120 °C for 6 h in a vacuum oven to obtain the final product (DSi).

Preparation of EP Samples: EP, EP-DSi_1 (with 1.0 wt.% DSi), EP-DSi_2 (with 2.0 wt% DSi), and EP-DSi_3 (with 3.0 wt.% DSi) were prepared, with the formulas listed in Table S1. DGEBA and DSi were mixed at 85 °C to form a transparent mixture, and then DDM was added and stirred vigorously for 15 min. The mixture was degassed for 3 min under vacuum and put into a preheated mold at 80 °C. The mixture was cured at 100 °C for 2 h, 120 °C for 2 h, and 150 °C for 4 h to obtain the EP-DSi sample. EP sample was prepared in the same way without the addition of DSi.

Characterizations: This section is presented in the Supporting Information.

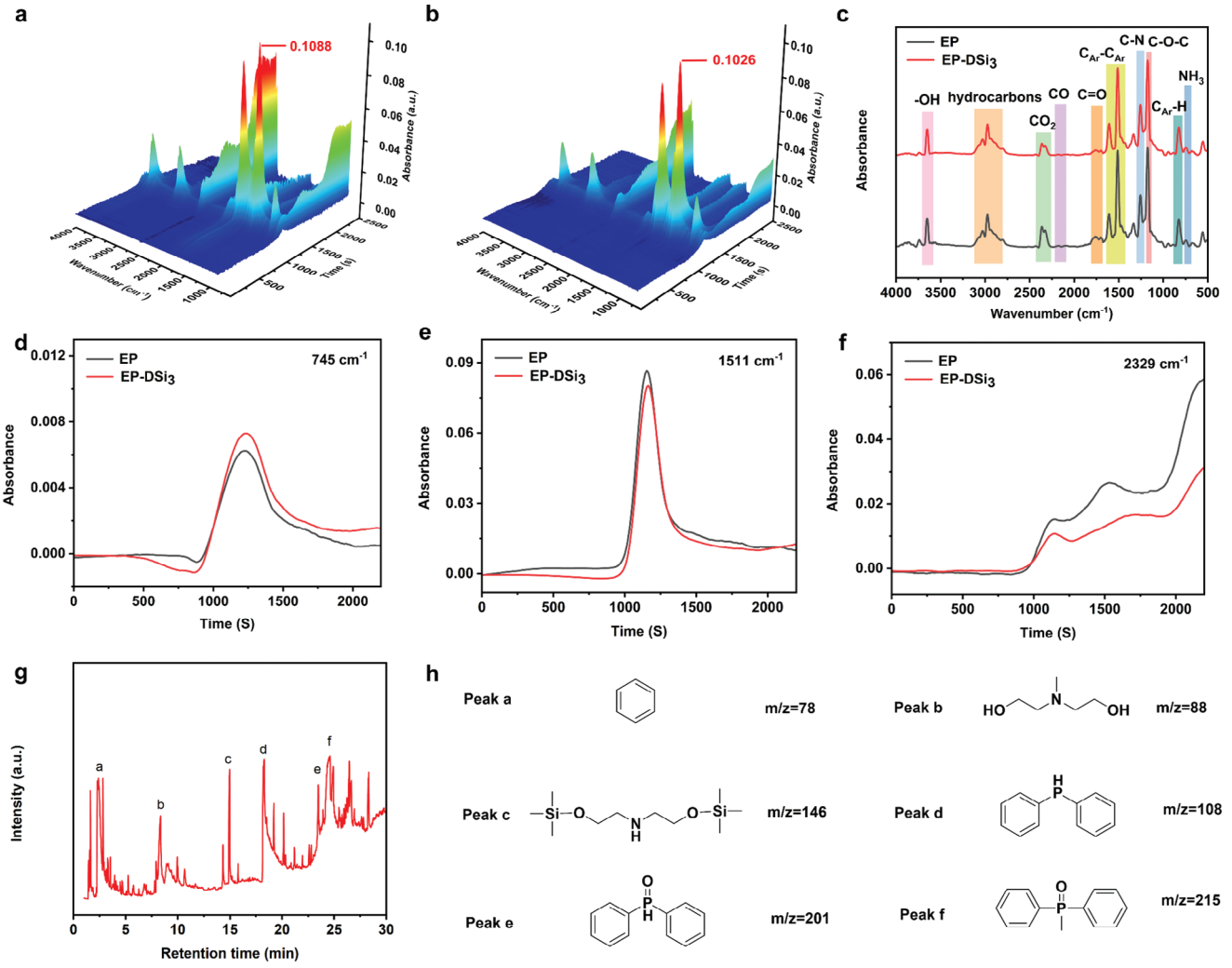

Figure 8. 3D FTIR curves of decomposition gaseous products for a) EP and b) EP-DSi_3, c) FTIR curves of decomposition gaseous products for EP and EP-DSi_3 at T_{max}, Absorbance versus temperature curves of EP and EP-DSi_3 at d) 745, e) 1511, and f) 2329 cm^{-1}, g) total ion chromatogram of DSi, and h) pyrolysis products of DSi detected by Py-GC/MS.

Supporting Information

Supporting Information is available from the Wiley Online Library or from the author.

Acknowledgements

This work was supported by the Australian Research Council (DE230100616).

Open access publishing facilitated by University of Southern Queensland, as part of the Wiley - University of Southern Queensland agreement via the Council of Australian University Librarians.

[Correction added on February 24, 2025, after first online publication: the funding statement has included in this version.]

Conflict of Interest

The authors declare no conflict of interest.

Data Availability Statement

The data that support the findings of this study are available from the corresponding author upon reasonable request.

Keywords

epoxy resin, hyperbranched polymer, multifunction

Received: October 10, 2024
Revised: October 28, 2024
Published online: November 11, 2024

[1] X. Li, J. Liang, T. Shi, D. Yang, X. Chen, C. Zhang, Z. Liu, D. Liu, Q. Zhang, *Ceram. Int.* **2020**, *46*, 12911.
[2] S. Huo, P. Song, B. Yu, S. Ran, V. S. Chevali, L. Liu, Z. Fang, H. Wang, *Prog. Polym. Sci.* **2021**, *114*, 101366.

[3] X. Bi, H. Di, J. Liu, Y. Meng, Y. Song, W. Meng, H. Qu, L. Fang, P. Song, J. Xu, *Adv. Compos. Hybrid Mater.* **2022**, *5*, 1743.
[4] L. He, T. Chen, Y. Zhang, L. Hu, T. Wang, R. Han, J. L. He, W. Luo, Z. G. Liu, J. N. Deng, M. J. Chen, *Composites, Part B* **2022**, *230*, 109553.
[5] J. Yang, H. Wang, X. Liu, S. Fu, P. Song, *Compos. Sci. Technol.* **2021**, *212*, 108884.
[6] M. Rajaei, D. Y. Wang, D. Bhattacharyya, *Composites, Part B* **2017**, *113*, 381.
[7] Z. Lin, W. Zhang, G. Lou, Z. Bai, J. Xu, H. Li, Y. Zong, F. Chen, P. Song, L. Liu, J. Dai, *Emerg. Manag. Sci. Technol.* **2023**, *3*, 21.
[8] H. Wang, J. Yuan, Y. Wang, Y. Ma, S. Lyu, Z. Zhu, *Polym. Degrad. Stab.* **2022**, *199*, 109909.
[9] J. Hu, L. Zhang, M. Chen, J. Dai, N. Teng, H. Zhao, X. Ba, X. Liu, *Polymers* **2023**, *15*, 449.
[10] K. Zhou, J. Liu, Y. Shi, S. Jiang, D. Wang, Y. Hu, Z. Gui, *ACS Appl. Mater. Interfaces* **2015**, *7*, 6070.
[11] G. Zhang, W. Wu, M. Yao, Z. Wu, Y. Jiao, H. Qu, *Mater. Des.* **2023**, *226*, 111664.
[12] T. Ma, C. Guo, *J. Anal. Appl. Pyrolysis* **2017**, *124*, 239.
[13] S. Tang, L. Qian, Y. Qiu, Y. Dong, *Polym. Degrad. Stab.* **2018**, *153*, 210.
[14] X. Tong, X. Dong, H. Jia, H. Li, X. Gu, J. Sun, S. Zhang, *Polym. Degrad. Stab.* **2024**, *227*, 110890.
[15] P. Zheng, H. Zhao, Q. Liu, *Polym. Degrad. Stab.* **2024**, *225*, 110817.
[16] H. Wang, S. Huo, C. Wang, G. Ye, Q. Zhang, P. Song, H. Wang, Z. Liu, *Prog. Org. Coat.* **2024**, *193*, 108562.
[17] G. Ye, S. Huo, C. Wang, Q. Zhang, B. Wang, Z. Guo, H. Wang, Z. Liu, *Sustainable Mater. Technol.* **2024**, *39*, e00853.
[18] X. Li, Q. Xie, J. Lin, J. Huang, K. Xie, J. Liu, X. Li, W. Wei, *J. Appl. Polym. Sci.* **2023**, *140*, e54474.
[19] M. Chai, H. Liu, Y. Wu, K. Xue, P. Zhang, L. Liu, Y. Huang, *Chem. Eng. J.* **2024**, *493*, 152785.
[20] M. Fang, J. Qian, X. Wang, Z. Chen, R. Guo, Y. Shi, *ACS Omega* **2021**, *6*, 7094.
[21] G. Yuan, B. Yang, Y. Chen, Y. Jia, *Composites, Part A* **2019**, *117*, 345.
[22] Q. Chen, S. Huo, Y. Lu, M. Ding, J. Feng, G. Huang, H. Xu, Z. Sun, Z. Wang, P. Song, *Small* **2024**, *20*, 2310724.
[23] X. Hu, H. Yang, Y. Jiang, H. He, H. Liu, H. Huang, C. Wan, *J. Hazard. Mater.* **2019**, *379*, 120793.
[24] W. Wang, Y. Liu, H. Wen, Q. Wang, *Polym. Degrad. Stab.* **2021**, *184*, 109479.
[25] Y. Tang, X. Zhang, X. Liu, W. Wei, X. Li, *Chem. Eng. J.* **2024**, *482*, 148992.
[26] Y. Xiao, Z. Jin, L. He, S. Ma, C. Wang, X. Mu, L. Song, *Composites, Part B* **2020**, *182*, 107616.
[27] J. Choi, K. H. Min, B. S. Kim, S. H. Baeck, S. E. Shim, Y. Qian, *Prog. Org. Coat.* **2024**, *186*, 108081.
[28] X. Zhang, T. Liu, Z. Liu, X. Zhu, C. Long, J. Li, Q. Gao, J. Li, P. Song, *Sustainable Mater. Technol.* **2024**, *40*, e00979.
[29] J. Li, H. Wang, S. Li, *Polym. Degrad. Stab.* **2019**, *164*, 36.
[30] C. Wan, H. Duan, C. Zhang, C. Liu, H. Zhao, H. Ma, *ACS Appl. Polym. Mater* **2023**, *5*, 1775.
[31] A. Bifulco, D. Parida, K. A. Salmeia, R. Nazir, S. Lehner, R. Stämpfli, H. Markus, G. Malucelli, F. Branda, S. Gaan, *Mater. Des.* **2020**, *193*, 108862.
[32] X. F. Liu, Y. F. Xiao, X. Luo, B. W. Liu, D. M. Guo, L. Chen, Y. Z. Wang, *Chem. Eng. J.* **2022**, *427*, 132031.
[33] F. Luo, K. Wu, S. Wang, M. Lu, *Compos. Sci. Technol.* **2017**, *144*, 100.
[34] Y. Feng, C. He, Y. Wen, Y. Ye, X. Zhou, X. Xie, Y. W. Mai, *Composites, Part A* **2017**, *103*, 74.
[35] J. Wang, C. Ma, P. Wang, S. Qiu, W. Cai, Y. Hu, *Polym. Degrad. Stab.* **2018**, *149*, 119.
[36] S. Huo, Z. Liu, C. Li, X. Wang, H. Cai, J. Wang, *Polym. Degrad. Stab.* **2019**, *163*, 100.
[37] S. Huo, Z. Zhou, J. Jiang, T. Sai, S. Ran, Z. Fang, P. Song, H. Wang, *Chem. Eng. J.* **2022**, *427*, 131578.
[38] G. Ye, S. Huo, C. Wang, P. Song, Z. Fang, H. Wang, Z. Liu, *Polym. Degrad. Stab.* **2023**, *207*, 110235.
[39] C. Wang, S. Huo, G. Ye, B. Wang, Z. Guo, Q. Zhang, P. Song, H. Wang, Z. Liu, *Composites, Part B* **2024**, *268*, 111075.
[40] J. Feng, Z. Ma, Z. Xu, H. Xie, Y. Lu, C. Maluk, P. Song, S. Bourbigot, H. Wang, *Chem. Eng. J.* **2022**, *431*, 134259.
[41] Z. Ma, J. Feng, S. Huo, Z. Sun, S. Bourbigot, H. Wang, J. Gao, L. C. Tang, W. Zheng, P. Song, *Adv. Mater.* **2024**, *36*, 2410453.
[42] S. Wang, B. Yu, K. Zhou, L. Yin, Y. Zhong, X. Ma, *J. Colloid Interface Sci.* **2019**, *550*, 210.
[43] R. J. Smith, K. M. Holder, S. Ruiz, W. Hahn, Y. Song, Y. M. Lvov, J. C. Grunlan, *Adv. Funct. Mater.* **2017**, *28*, 1703289.
[44] Z. Zhang, J. Qin, W. Zhang, Y. T. Pan, D. Y. Wang, R. Yang, *Chem. Eng. J.* **2020**, *381*, 122777.
[45] Y. Zhang, L. Liu, M. Yao, J. Feng, Y. Xue, P. K. Annamalai, V. Chevali, T. Dinh, Z. Fang, H. Liu, P. Song, *Chem. Eng. J.* **2024**, *495*, 153429.
[46] G. Tang, L. Zhou, P. Zhang, Z. Han, D. Chen, X. Liu, Z. Zhou, *J. Therm. Anal. Calorim.* **2019**, *140*, 625.
[47] G. Ye, S. Huo, C. Wang, Q. Zhang, H. Wang, P. Song, Z. Liu, *Small* **2024**, 2404634.
[48] J. Wang, J. Wang, S. Yang, X. Chen, K. Chen, G. Zhou, X. Liu, L. Xu, S. Huo, P. Song, H. Wang, *Chem. Eng. J.* **2024**, *485*, 149852.
[49] C. Schmidt, M. Ciesielski, L. Greiner, M. Döring, *Polym. Degrad. Stab.* **2018**, *158*, 190.
[50] W. Peng, S.-b. Nie, Y. Xu, W. Yang, *Polym. Degrad. Stab.* **2021**, *193*, 109715.
[51] Q. Shi, S. Huo, C. Wang, G. Ye, L. Yu, Z. Fang, H. Wang, Z. Liu, *Polym. Degrad. Stab.* **2022**, *203*, 110065.
[52] Y. Qi, D. Bao, X. Huan, Q. Xu, S. Ma, S. Qin, C. Gao, X. Hou, Y. Zhang, Z. Wen, *Polym. Degrad. Stab.* **2024**, *226*, 110833.
[53] X. Wang, T. Chen, J. Hong, W. Luo, B. Zeng, C. Yuan, Y. Xu, G. Chen, L. Dai, *Composites, Part B* **2020**, *200*, 108271.
[54] Q. Yang, J. Wang, X. Chen, S. Yang, S. Huo, Q. Chen, P. Guo, X. Wang, F. Liu, W. Chen, P. Song, H. Wang, *Chem. Eng. J.* **2023**, *468*, 143811.
[55] Y. Xue, M. Zhang, S. Huo, Z. Ma, M. Lynch, B. T. Tuten, Z. Sun, W. Zheng, Y. Zhou, P. Song, *Adv. Funct. Mater.* **2024**, 202409139.

